Experimental study on formation and decomposition characteristics of tetrahydrofuran and methane hydrate based on microfluidic chip technology

Jianyu Yang & Yuze Wang
Southern University of Science and Technology, Shenzhen, CHN

ABSTRACT: Gas hydrates are considered a promising energy source for the 21st century, and understanding their formation and decomposition processes is crucial. This study utilized micro-fluidic technology to observe the secondary formation and decomposition of hydrates at the pore scale, comparing methane-tetrahydrofuran(THF)-water and methane-water systems. The study found that hydrates tended to form and decompose at the gas-liquid interface, and the second formation rate of hydrates was higher than the first. During depressurization, hydrates located at the solid-liquid interface decomposed first, followed by decomposition towards the interior of the hydrate. The study sheds light on the formation and decomposition characteristics of gas hydrates at the pore scale, providing some insights for the safe and efficient exploitation of gas hydrate.

1 **Introduction**

Natural gas hydrate is a compound consisting of cage-like structures formed by the combination of hydrocarbon gases, such as methane, and water under conditions of high pressure and low temperature. Due to its extensive distribution, substantial reserves, high combustion value, and environmentally friendly production process, it has been touted as a promising strategic replacement for traditional energy sources in the 21st century. Many countries have conducted successful natural gas hydrate trial extractions, but these extractions have exposed various challenges, such as severe sand production during production and low methane gas production rates that fail to meet commercial demand. Thus, exploring the formation and decomposition characteristics and mechanisms of natural gas hydrates at the pore scale is crucial for the on-site extraction of natural gas hydrates.

In recent years, microfluidic chip technology has become increasingly utilized for investigating the pore distribution and phase transition processes of natural gas hydrates. This technology provides advantages such as the real-time visualization and observation of multi-component substance interactions in micro-pores (Tohidi, Anderson et al., 2001; Kang, Yun et al., 2016; Li, Zhang et al., 2022; Xu, Kou et al., 2023; Zhang, Zhang et al., 2023). Furthermore, it has been employed for measuring changes in permeability of porous media during gas hydrate phase transitions (Chen, Sun et al., 2019; Chen, Gao et al., 2020; Ji, Hou et al., 2021) and establishing kinetic models for gas hydrate formation and decomposition (Chen, Pinho et al., 2017; Chen and Hartman, 2018; Li, Wang et al., 2021).

Microfluidic chip technology has emerged as a powerful tool for in-situ and real-time observation of hydrate formation and decomposition at the pore scale, enabling investigations into their underlying patterns. Wang et al.(Wang, Cheng et al. 2021) utilized microfluidic technology to examine the formation and growth of methane hydrate, as well as local reformation induced by microbubble aggregation. Their study proposed four hydrate growth modes, including accumulation growth of hydrate film in the channel, diffusion growth in narrow throat channels, contraction of isolated gas bubbles, and gas channels with entangled hydrate film. Similarly, Ji et al. (Ji, Hou et al. 2021) found that methane hydrate formation only occurred at the gas-liquid interface, with excess liquid phase conditions leading to generation towards the gas phase. Local hydrate exhibited secondary formation after dissociation during the formation process. Lv et al.(Lv, Xue et al. 2021) explored xenon hydrate formation and dissociation under various salinities through microfluidic chips. Their study revealed that the growth process of hydrate can be divided into four stages: induction stage, preliminary nucleation of hydrate, rapid nucleation of hydrate, and nucleation maturation of hydrate. Increasing salinity reduced the surface hydrophilicity of hydrate. Li et al.(Li, Wang et al. 2022) investigated methane hydrate formation and decomposition processes in methane-pure water and methane-salt water systems using microfluidic technology. Their study found that large bubbles in pores would generate a layer of hydrate shell enveloping methane gas, while small bubbles would be completely consumed by the growth of hydrate to produce stable transparent crystal hydrate that was not easily decomposed. Chen et al.(Chen, Sun et al. 2019) conducted a study which revealed that the initial dissociation stage of methane hydrate does not solely lead to the production of water and gas, but also results in the generation of small fragments of hydrate. Similarly, Li et al. (Li, Liu et al., 2023) identified that the process of pressure reduction decomposition can be categorized into three distinct stages. Initially, the reduction of pressure results in the disturbance of the outer shell of the hydrate, followed by the reaction of methane present inside the shell with water, generating new hydrate. Subsequently, the pressure experiences a slight change, which is followed by the onset of decomposition. During this stage, the pressure drops linearly, accompanied by intense gas-water migration. It is noteworthy that the reduction in pressure causes the fracture of the outer shell of the hydrate, leading to the release of methane, which can have significant implications for the environment.

Microfluidic chip technology offers a promising approach to examining the spatial distribution and growth pattern of hydrate formation in pores. Tohidi et al.(Tohidi, Anderson et al. 2001) observed through microfluidic experiments that hydrate formation primarily occurred at the center of the pore space. Similarly, Kang et al.(Kang, Yun et al. 2016) noted that tetrahydrofuran hydrate crystals were initially dispersed throughout the pore space and eventually merged to form larger crystals. Li et al.(Li, Zhang et al. 2022) conducted further investigations on the effect of initial gas-water saturation on the growth characteristics and existence form of hydrate. Their findings revealed that when water served as the initial continuous phase, hydrate growth was directed towards the center of the pore. However, when gas was the initial continuous phase, hydrate grew along the pore wall, towards the center of the pore. Additionally, Xu et al.(Xu, Kou et al. 2023) examined the impact of gas-liquid interface perturbations on hydrate formation and demonstrated that constant-pressure flow perturbations in random pore structures are the most effective means of generating hydrate. Furthermore, Zhang et al.(Zhang, Zhang et al. 2023) investigated the formation and plugging of hydrate under different gas-liquid flow conditions and found that an increased number of pore channel intersections and higher pore pressure could make the pore more susceptible to blockage.

Currently, microfluidic research on gas hydrate primarily focuses on the initial formation and decomposition process of hydrate in the tetrahydrofuran (THF)-water system or methane-water system. However, there is a scarcity of studies on the secondary formation and decomposition of hydrate and the variations in formation and decomposition characteristics of hydrate between the two systems. The liquid-phase hydrate products resulting from decomposition in the THF-water system cannot fully replicate the process of hydrate decomposition that releases methane. Therefore, this paper introduces methane into the THF-water system and utilizes microfluidic technology to investigate the secondary formation and decomposition process of hydrate in the methane-tetrahydrofuran-water system, with the aim of exploring the secondary formation and decomposition characteristics of hydrate. The formation and decomposition process of hydrate in both methane-tetrahydrofuran-water and methane-water systems will also be observed to examine the differences in formation and decomposition processes of hydrate between the two systems. These findings are crucial for promoting an understanding of the microscopic mechanisms governing hydrate formation and decomposition, and for facilitating the development of natural gas hydrate exploitation.

2 Material and methods

2.1 Experimental equipment and materials

This paper employs a custom-built microfluidic experimental device, operating under high-pressure and low-temperature conditions, to conduct experiments. The device comprises an injection system, surrounding pressure system, temperature control system, collection system, optical microscope observation system, and sensor data acquisition system. The device connection diagram is presented in Fig.1. The experimental materials consist of deionized water, methyl blue, tetrahydrofuran, and methane gas.

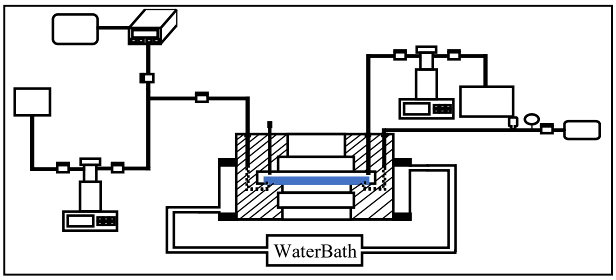

Fig.1: Experimental device

2.2 Experimental procedure

Tetrahydrofuran (THF) is recognized for its ability to lower the pressure threshold required for hydrate formation, reduce induction times, and increase the rate of hydrate formation. Consequently, it is commonly employed to accelerate the formation of gas hydrate (Iida, Mori et al. 2001). To achieve rapid formation and decomposition of hydrate, our research group investigated the secondary formation and decomposition of hydrate using a 20% THF solution. Normally, a 20% THF-water system produces type II tetrahydrofuran hydrate, which has a molecular structure of 8 THF·136 H_2O (Gough and

Davidson 1971). In this study, methane gas was introduced to observe the process of methane release during hydrate decomposition in the pores of the observation chip. In a methane-20% THF-water system, type II hydrate was formed, which has a molecular structure of $16\ CH_4 \cdot 8\ THF \cdot 136\ H_2O$ (Subramanian and Sloan Jr 1999, Sharma, Sowjanya et al. 2014, Dong, Sun et al. 2015).

In this study, experiments were conducted to synthesize and decompose methane hydrate in both methane-THF-water and methane-water systems using the setup previously described. Multiple synthesis and decomposition experiments of methane-THF-water hydrate were performed as follows: a 20% THF aqueous solution was mixed with a specific amount of methane, and the resulting mixture was injected into a microfluidic chip for synthesis under conditions of 2℃ and 3.5 MPa. After completion of synthesis, the hydrates were decomposed under conditions of 20℃ and 3.5 MPa. The hydrates were then synthesized for a second time under the same conditions, followed by a second decomposition under conditions of 20℃ and 3.5 MPa. In the case of methane-water hydrate, the following steps were taken for the synthesis and decomposition experiments: a specific amount of methane gas was mixed with water and injected into a microfluidic chip for hydrate formation under conditions of 2℃ and 8 MPa. After complete formation, the hydrates were decomposed by reducing the pressure to 2 MPa under conditions of 2℃. Overall, the results of these experiments provide valuable insights into the synthesis and decomposition of methane hydrate in both methane-THF-water and methane-water systems, and can inform future research in this area.

2.3 *Image-processing method*

The formation of gas hydrate inside the microfluidic chip can present challenges when attempting to accurately distinguish between the hydrate and the liquid phase. Although both the hydrate and liquid phase inside the microfluidic chip may appear transparent to the naked eye, microscopic observation reveals that there is still a significant problem in accurately identifying and distinguishing between water and gas hydrate (Li, Wang et al. 2021). To address this challenge, Tohidi and Tacker (Tohidi, Anderson et al. 2001, Tacker 2016) utilized the characteristic of liquid phase dyes being expelled during the formation of gas hydrate to distinguish between hydrate and liquid phase water. Therefore, in this study, methylene blue was introduced as a dye to more accurately distinguish and identify hydrate and liquid phase water, as illustrated in Fig. 2. A comparison of Fig. 2 shows that after the addition of the dye, the initial gas and liquid phase distribution can be more easily observed and distinguished. Without the dye, it was challenging to observe anything beyond the outer shell of the hydrate in the microfluidic chip, and hydrate generated in the liquid phase was not observable. However, after the addition of the dye, the microfluidic chip can simultaneously observe the outer shell of the hydrate and the hydrate generated in the liquid phase. With the subsequent threshold segmentation processing, the gas hydrate, liquid phase water, and pore space can be more effectively separated and analyzed. Overall, the use of methylene blue as a dye in this study provides an improved method for accurately identifying and distinguishing between hydrate and liquid phase water during the formation of gas hydrate inside the microfluidic chip, which can inform future research in this area.

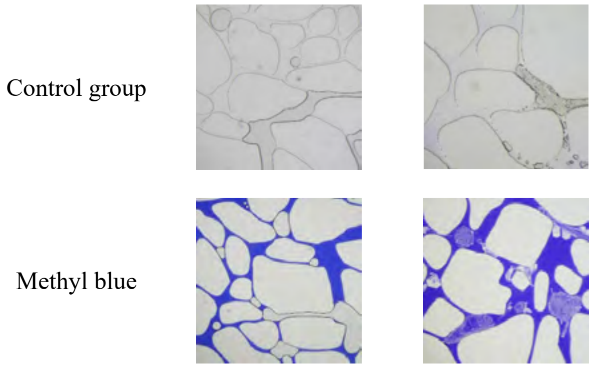

Fig.2 Comparison of the effect of adding Methyl blue

The incorporation of methylene blue into microfluidic chips provides a means to generate gas hydrate, which can then be extracted and analyzed using a threshold segmentation method to measure hydrate saturation. An example micrograph of gas hydrate formed after dye addition is shown in Fig. 3a. Through subsequent binarization processing (Fig. 3b), two-dimensional distribution maps of gas hydrate (Fig. 3c) and pores (Fig. 3d) can be obtained. By using ImageJ to analyze the area of gas hydrate and pores separately, the corresponding hydrate saturation can be calculated according to the definition of hydrate saturation. This approach provides a reliable and effective method for measuring hydrate saturation within the microfluidic chip.

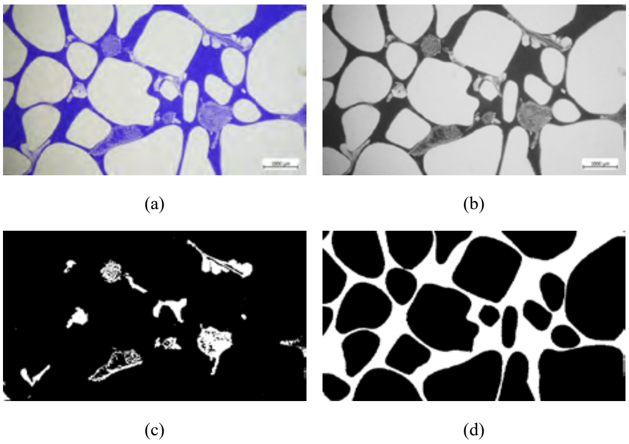

(a) (b) (c) (d)

Fig.3: Threshold segmentation of natural gas hydrate (a) initial image; (b) binary gray level map; (c) gas hydrate; (d) Pore

3 Characteristics of secondary hydrate formation and decomposition in methane - THF- water system

In the methane-THF-water system, hydrates preferentially form at the gas-liquid interface during the two-stage hydrate formation process, growing towards the gas phase. The distribution of methane, pore particles, and water before the first and second synthesis of the methane-THF-water system can be clearly distinguished using the microfluidic chip, allowing for observation of the gas-liquid contact position (Fig. 4a I, Fig. 4b I). When the system is at 2 ℃ and 3.5 MPa, hydrates are preferentially formed at the gas-liquid contact interface during both the first and second hydrate formation processes (Fig. 4a II, Fig. 4b II). As hydrates form, the gas phase gradually darkens from gray to black (Fig. 4a III, Fig. 4b III). Further synthesis of hydrates leads to the gradual disappearance of the residual liquid phase in the microfluidic chip (Fig. 4a IV, Fig. 4a V, Fig. 4b IV, Fig. 4b V). In the later stages of the two-stage hydrate formation process, hydrate redistribution occurs in the microfluidic chip, where local hydrates decompose and form (Fig. 4a VI, Fig. 4b VI).

This study provides insights into the preferential formation of hydrate at the gas-liquid interface and the occurrence of a secondary distribution phenomenon during the hydrate formation process. These findings are in line with previous research by Wang, Cheng et al. (2021) and Li, Wang et al. (2022). The lower Gibbs free energy for hydrate nucleation at the gas-liquid interface, combined with the adsorption and dissolution processes, promotes the concentration of guest molecules at the interface, thereby facilitating hydrate formation (Sloan and Koh, 2007). In the early stages of hydrate formation, the rapid formation factors, including high pressure, low temperature, and suitable solute concentrations, enhance the interaction between water and gas molecules, thereby promoting hydrate formation. However, the hydrate formed in this stage typically exhibit relatively high energy and unstable structures (Fig. 4a V Red box). As time progresses, the structure and energy of the hydrate change, and the initial hydrate formed may not satisfy the principle of minimum Gibbs free energy, resulting in decomposition (Fig. 4a V compared to Fig. 4a VI Red box). The decomposed gas and water molecules recombine to form more stable hydrate, and during the redistribution of hydrate, the structure and energy of the hydrate gradually approach stability, ultimately reaching equilibrium. Moreover, this study reveals that the amount of redistributed hydrate seems to depend on the initial water content, with a higher initial water content leading to a larger area of redistributed hydrate. Further investigations are required to explore the relationship between the amount of redistributed hydrate and the initial water content in future studies.

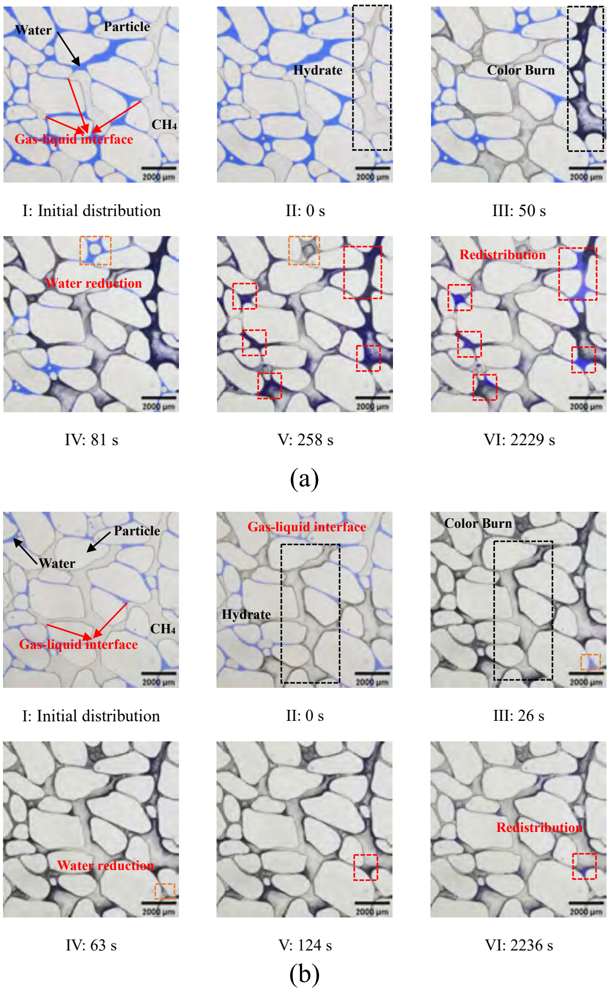

Figure 4: Hydrate formation process in methane-THF-water system (a) the first formation; (b) The second formation

The decomposition process of hydrate in the methane-THF-water system can be categorized into several stages. Firstly, hydrate located at the gas-liquid interface undergoes decomposition, resulting in the production of water that subsequently combines with the dye to form a blue liquid phase distributed at the gas-liquid interface (Fig. 5a I, II and Fig. 5b I, II). Secondly, as hydrate continue to decompose, isolated gas bubbles emerge in the pores (Fig. 5a III, Fig. 5b III). Thirdly, the formation of a connected gas phase occurs as a large number of isolated gas bubbles come into contact, and subsequently traverse through the pores (Fig. 5a IV, V, VI and Fig. 5b IV). Fourthly, once the hydrate are entirely decomposed, small gas bubbles can easily form at locations with high initial saturation. Some of these small bubbles may conglomerate into larger bubbles, while many small bubbles persist (Fig. 5a VII, VIII and Fig. 5b V, VI).

Clathrate hydrates exhibit lower Gibbs free energy at the gas-liquid interface, but they are more vulnerable to temperature and pressure changes from the external environment (Sloan and Koh, 2007). As a result, at temperatures exceeding the hydrate decomposition threshold, clathrates located at the gas-liquid interface decompose preferentially, leading to the release of significant amounts of methane at sites where clathrate saturation is high. Due to the constraints of pore space, a multitude of micro methane bubbles are formed (Fig. 5a VII, Fig. 5b VI). Bubble formation is influenced by surface tension and viscosity. Lower surface tension results in weaker intermolecular forces, facilitating bubble formation. Conversely, higher viscosity increases frictional forces between liquid molecules, impeding bubble formation. Tetrahydrofuran, a polar organic solvent, has lower viscosity and surface tension than water, and thus, the decomposition of clathrates in the methane-THF-water system yields a vast number of small microbubbles.

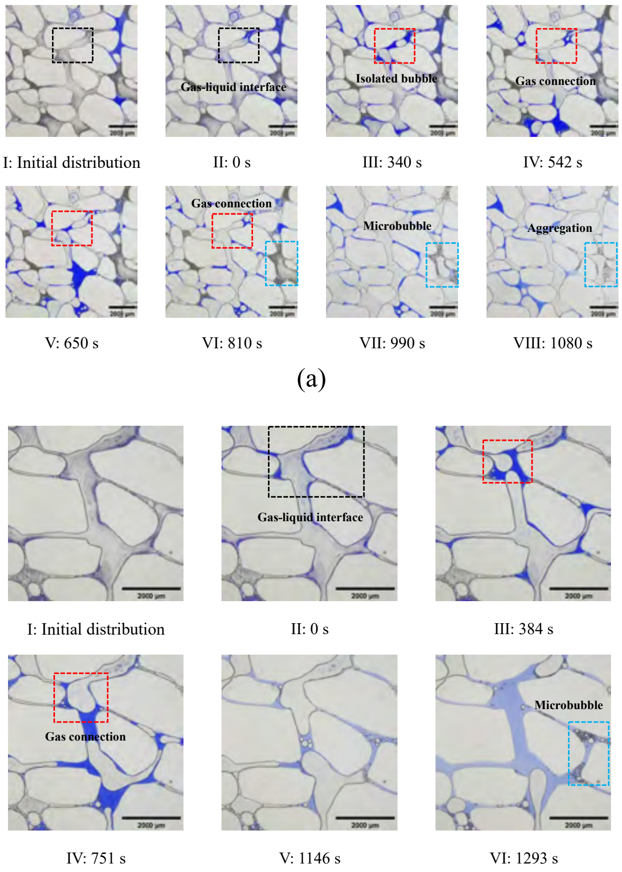

(a)

(b)

Fig.5 Hydrate decomposition process in methane-THF-water system (a) the first decomposition; (b) The second decomposition

The clathrate memory effect plays a significant role in the formation rate, but has a negligible impact on the decomposition rate. In the methane-THF-water system, the secondary formation rate of clathrates is considerably higher than the initial formation rate, and the final saturation is maintained at around 63% after the complete formation of clathrates (Fig. 6a). The secondary decomposition rate of clathrates in the methane-THF-water system is essentially consistent with the initial decomposition rate (Fig. 6b). Initial clathrate formation necessitates overcoming nucleation barriers and growth resistance, whereas secondary formation can accelerate the nucleation and growth process by utilizing microstructures or memory effects in residual water. Thus, under the same formation conditions, the memory effect results in a faster secondary formation rate of clathrates.

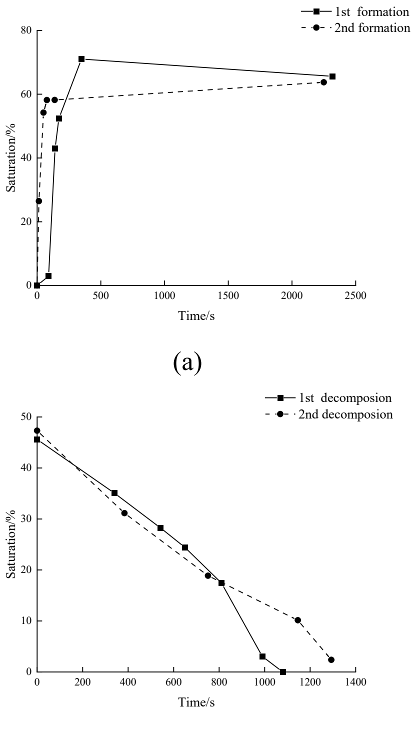

(a)

(b)

Fig.6 Hydrate saturation curve with time in methane-THF-water system (a) Hydrate saturation of the first and second formation; (b) Hydrate saturation of the first and second formation decomposition

Hence, the characteristics of first and second hydrate formation in the methane-THF-water system are similar: hydrates are initially formed at the gas-liquid interface and subsequently grow towards the gas phase, while undergoing hydrate redistribution during the late growth stage. Similarly, the characteristics of first and second hydrate decomposition in the methane-THF-water system are consistent: hydrates at the gas-liquid interface tend to decompose preferentially, generating isolated gas bubbles that then coalesce into a connected gas phase, migrating within the pore space, and eventually leading to complete hydrate decomposition. In areas with a high initial saturation, the formation of microbubbles is more probable. Furthermore, although the second formation hydrate decomposition rate is comparable to the first formation rate, the second formation hydrate formation rate is significantly higher owing to the presence of hydrate memory effects, indicating that multiple hydrate formation processes do not influence the hydrate decomposition rate. Additional research is necessary to investigate the impact of hydrate formation and decomposition history on hydrate formation and decomposition rates.

During the actual production, the temperature of the reservoir's local area tends to decrease because of the decomposition of gas hydrates. The immediate vicinity of wellbore with low temperature is prone to secondary generation of hydrates, blocking the porous medium flow channels. The efficiency of gas hydrate extraction decreases due to the low permeability of reservoir. Moreover, the gas produced by the decomposition of hydrates accumulates in the pores. The surge of pressure in pores might cause the overburden of the reservoir to break. Consequently, a large amount of methane leaks into the ocean and atmosphere, resulting in geological landslides, ocean anoxia, and the greenhouse effect.

4 Characteristics of hydrate formation and decomposition in methane-water system

Type I clathrate hydrate is a common occurrence in methane-water systems (Subramanian and Sloan Jr, 1999). To gain a better understanding of the formation and decomposition of gas hydrates under field conditions, this study utilized microfluidic technology to observe the process of clathrate hydrate formation in methane-water systems under a microscope, as illustrated in Figure 7.

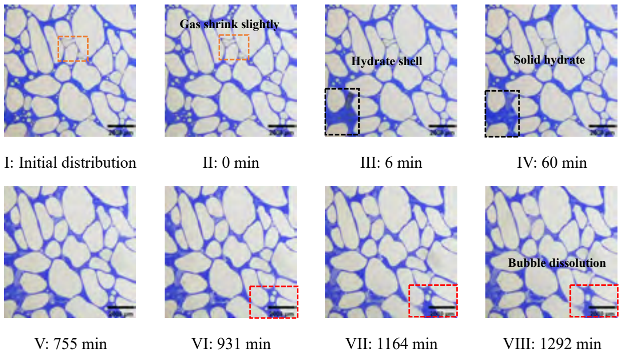

I: Initial distribution II: 0 min III: 6 min IV: 60 min

V: 755 min VI: 931 min VII: 1164 min VIII: 1292 min

Fig.7 The formation of methane hydrate

Similar to the methane-THF-water system, clathrate hydrate formation in the methane-water system primarily occurs at the gas-liquid interface. The process of methane hydrate formation in this system can be divided into several stages: (1) placing the methane-water system under equilibrium conditions leads to the dissolution of some methane gas phase in the pore of the chip into water, resulting in a slight reduction in gas phase area (Fig. 7 I, II); (2) after the induction period of hydrate formation, methane hydrate preferentially forms at the gas-liquid interface, resulting in the formation of a single layer of hydrate shell encapsulating the methane gas. Due to the gas's effect on transparency, the entire hydrate shell appears black (Fig. 7 III); (3) mass transfer occurs through the hydrate shell, and the hydrate shell grows inward towards the gas phase, gradually forming a white solid clathrate hydrate (Fig. 7 IV). This result is consistent with the findings of Zhang et al. (Zhang, Zhang et al. 2023); (4) in the later stage of hydrate formation, the remaining small gas bubbles in the liquid phase gradually dissolve, promoting nearby hydrate crystals to grow towards the liquid phase (Fig. 7 V, VI, VII).

During the formation of the methane-THF-water system, no significant gas dissolution process was observed. This phenomenon may be attributed to the introduction of THF, which facilitates hydrate formation and promotes direct reaction of a large quantity of free methane gas with water to form hydrate. Furthermore, the liquid content of the methane-THF-water system is relatively low, resulting in a limited volume of dissolved gas that is not readily observable under a microscope.

The process of methane hydrate decomposition in the methane-water system can be broken down into several stages. Firstly, methane hydrate decomposes preferentially at the gas-liquid contact interface, resulting in the formation of isolated gas bubbles. Subsequently, as the decomposition progresses, numerous isolated gas bubbles merge, giving rise to a connected gas phase which constitutes the decomposition region (Figure 8 I). Finally, the connected gas phase within the pore migrates in the same direction as the propagation direction of the hydrate decomposition zone. In comparison with the solid-liquid interface, the hydrate at the solid-gas interface are more susceptible to decomposition (Figures 8 II, III, IV, V). This is due to the relatively weak interaction force between gas molecules and solid molecules, in contrast to the relatively strong interaction force between liquid molecules and solid molecules. Overcoming the relatively small interaction force is necessary to form and detach the gas-solid interface.

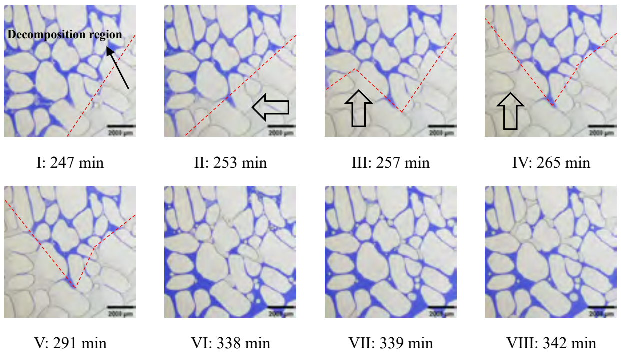

I: 247 min II: 253 min III: 257 min IV: 265 min

V: 291 min VI: 338 min VII: 339 min VIII: 342 min

Fig.8 The decomposition of methane hydrate

During the process of methane hydrate formation, two types of hydrate are generated: filling block hydrate and dispersed point hydrate. The former is formed by the dissolution of methane gas in the liquid phase and water, resulting in a slower formation rate due to the methane dissolution process (Figure 9a). The latter is formed by the reaction of free methane gas and water, resulting in a faster formation rate (Figure 9b). In the formation process of the microfluidic chip, a combination of the two types of hydrate was observed (Figure 9c). This may be attributed to the rapid reaction of free methane gas with the liquid phase to form a hydrate shell in the initial stage of hydrate formation, concurrent with the dissolution of methane gas. Upon reaching the saturation of the dissolved methane gas in the liquid phase, nucleation and growth occur at the already formed hydrate shell, leading to the combination of the two types of hydrate.

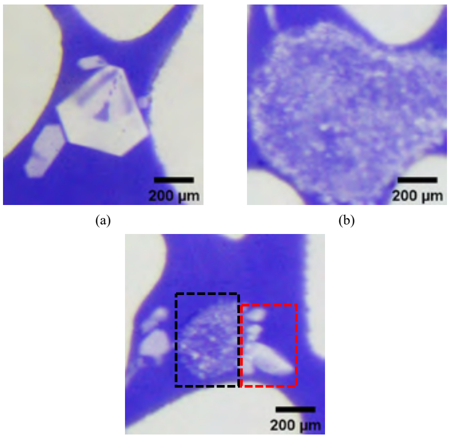

(a) (b) (c)

Fig.9 Form of methane hydrate (a) block hydrate; (b) dispersed point hydrate; (c) Combination

The characteristics of hydrate formation and dissociation in the methane-THF-water and methane-water systems are essentially the same. During formation, hydrates are preferentially formed at the gas-liquid interface and continue to grow in the direction of the gas phase. During dissociation, hydrates at the gas-liquid interface are preferentially dissociated, generating isolated gas bubbles that merge to form a continuous gas phase, driving fluid migration and hydrate dissociation. However, some differences exist between the two systems. The introduction of THF significantly reduces the formation time of methane-THF-water hydrates compared to methane-water hydrates. In the methane-water system, two types of hydrate crystals are observed, while in the methane-THF-water system, only one type is observed. This is due to the slower formation of hydrates in the methane-water system and the different forms of hydrate crystals generated by free and dissolved gases. In the methane-THF-water system, the formation rate of hydrates is extremely fast, and the amount of dissolved methane is very low during the formation process. As a result, a large amount of free gas can rapidly form hydrates with water, leading to the eventual formation of only one type of natural gas hydrate.

During the later stages of hydrate formation, a phenomenon known as hydrate redistribution is observed in the methane-THF-water system after 30 minutes of stable hydrate formation (approximately 8 times the formation time). However, this phenomenon is not observed in the methane-water system. This may be attributed to the slower formation of methane hydrate in the methane-water system, which takes about a day to fully form. The phenomenon of methane hydrate redistribution can only be observed after approximately a week. Upon dissociation, the methane-THF-water system produces a substantial number of micro gas bubbles, while the methane-water system produces almost none. The addition of THF reduces the surface tension and viscosity of the fluid, making it easier for fine micro gas bubbles to form after hydrate dissociation. Overall, these observations suggest that the presence of THF can significantly impact the formation and dissociation of methane hydrates in water systems. These findings highlight the importance of considering the role of additives in the study of hydrate behavior and provide insight into the potential implications of such phenomena in real-world applications.

The pressure of reservoir increases rapidly because of the extraction of hydrates. If the pore pressure cannot be controlled in time, it may lead to equipment damage, low extraction rate, and geological fractures. However, by understanding of the generation and decomposition mechanisms of hydrates, we can better predict and control these changes based on pressure, temperature, and fluid properties, adjust extraction plans promptly, and ensure production safety and economic benefits.

5 Conclusions

This article investigates the secondary formation and decomposition of hydrates in the methane-tetrahydrofuran-water system using microfluidic chips. The study compares the formation and decomposition characteristics of hydrates in the methane-tetrahydrofuran-water and methane-water systems and explores the differences between the two systems. The main findings of this research are summarised as follows:

(1) The first and second formation of hydrates in the methane-THF-water system exhibit consistent characteristics. Hydrates are predominantly formed at the gas-liquid interface and grow towards the gas phase. A phenomenon of hydrate redistribution is observed during the late growth stage.

(2) The first and second decomposition of hydrates in the methane-THF-water system also exhibit consistent characteristics. Hydrates at the gas-liquid interface preferentially decompose, producing isolated gas bubbles. These bubbles converge to form a connected gas phase, which moves within the pore, leading to the complete decomposition of hydrates. Regions with high initial saturation are conducive to the generation of micro-sized bubbles.

(3) The hydrate memory effect results in a significantly higher formation rate of secondary hydrates compared to the first formation, while the decomposition rate of secondary hydrates is similar to that of the first formation. These results suggest that multiple formations of hydrates do not significantly affect the decomposition rate of hydrates.

(4) Two types of hydrates are generated in the methane-water system. The first type is a block-shaped hydrate formed by methane dissolved in liquid and water. The second type is a dispersed point-shaped hydrate formed by free methane gas and water.

(5) The formation and decomposition characteristics of hydrates in the methane-THF-water and methane-water systems are essentially the same. During formation, hydrates are primarily generated at the gas-liquid interface and continue to grow along the gas phase. During decomposition, hydrates at the gas-liquid interface preferentially decompose, producing isolated gas bubbles, which then converge to form a continuous gas phase. This process drives fluid migration and hydrate decomposition.

(6) Understanding the mechanism of initial gas hydrate exploitation and decomposition is important to adjust the real-time exploitation scheme and improve efficiency during production. In addition, further research on secondary generation and decomposition mechanisms of gas hydrates plays a vital role in resolving blockages caused by secondary generation hydrates near the well and preventing geological disasters.

Acknowledgements

Authors acknowledge the financial support of Natural Science Foundation of China (Grant No. 52171262, 42141003) and Science and Technology Innovation Committee of Shenzhen (Grant No. JCYJ20210324103812033) for conducting this study.

References

Chen, W. and R. L. Hartman (2018). 'Methane hydrate intrinsic dissociation kinetics measured in a microfluidic system by means of in situ Raman spectroscopy.' Energy & fuels 32(11): 11761-11771.

Chen, W., B. Pinho and R. L. Hartman (2017). 'Flash crystallization kinetics of methane (sI) hydrate in a thermoelectrically-cooled microreactor.' Lab on a Chip 17(18): 3051-3060.

Chen, Y., Y. Gao, N. Zhang, L. Chen, X. Wang and B. Sun (2020). 'Microfluidics application for monitoring hydrate phase transition in flow throats and evaluation of its saturation measurement.' Chemical Engineering Journal 383: 123081.

Chen, Y., B. Sun, L. Chen, X. Wang, X. Zhao and Y. Gao (2019). 'Simulation and observation of hydrate phase transition in porous medium via microfluidic application.' Industrial & Engineering Chemistry Research 58(12): 5071-5079.

Dong, Q., Y. Sun, W. Su and J. Liu (2015). 'Hydrate Formation and Decomposition of CH4 and N2 in Ordered Mesoporous Carbon CMK-3 in the Presence of Tetrahydrofuran.' Journal of Chemical & Engineering Data 60(5): 1318-1323.

Gough, S. and D. Davidson (1971). 'Composition of tetrahydrofuran hydrate and the effect of pressure on the decomposition.' Canadian Journal of Chemistry 49(16): 2691-2699.

Iida, T., H. Mori, T. Mochizuki and Y. H. Mori (2001). 'Formation and dissociation of clathrate hydrate in stoichiometric tetrahydrofuran–water mixture subjected to one-dimensional cooling or heating.' Chemical engineering science 56(16): 4747-4758.

Ji, Y., J. Hou, E. Zhao, C. Liu, T. Guo, Y. Liu, B. Wei and Y. Bai (2021). 'Pore-scale study on methane hydrate formation and dissociation in a heterogeneous micromodel.' Journal of Natural Gas Science and Engineering 95: 104230.

Kang, D. H., T. S. Yun, K. Y. Kim and J. Jang (2016). 'Effect of hydrate nucleation mechanisms and capillarity on permeability reduction in granular media.' Geophysical Research Letters 43(17): 9018-9025.

Li, S., N. Zhang, Z. Hu, D. Wu and L. Chen (2022). 'Visual experimental study on hydrate occurrence patterns and growth habits in porous media.' Chemical Engineering Science 262: 117971.

Li, X., M. Liu, Q. Li, W. Pang, G. Chen and C. Sun (2023). 'Visual study on methane hydrate formation and depressurization-induced methane hydrate dissociation processes in a micro-packed bed reactor.' Fuel 332: 125980.

Li, X., C. Wang, Q. Li, Q. Fan, G. Chen and C. Sun (2021). 'Study on the growth kinetics and morphology of methane hydrate film in a porous glass microfluidic device.' Energies 14(20): 6814.

Li, X., C. Wang, Q. Li, W. Pang, G. Chen and C. Sun (2022). 'Experimental observation of formation and dissociation of methane hydrate in a micromodel.' Chemical Engineering Science 248: 117227.

Lv, J., K. Xue, Z. Zhang, Z. Cheng, Y. Liu and H. Mu (2021). 'Pore-scale investigation of hydrate morphology evolution and seepage characteristics in hydrate bearing microfluidic chip.' Journal of Natural Gas Science and Engineering 88: 103881.

Sharma, D., Y. Sowjanya, V. D. Chari and P. Prasad (2014). 'Methane storage in mixed hydrate with tetrahydrofuran.'

Sloan and Koh, C. (2007). Clathrate hydrate of natural gases, thrid edition.

Subramanian, S. and E. Sloan Jr (1999). 'Molecular measurements of methane hydrate formation.' Fluid Phase Equilibria 158: 813-820.

Tacker, M. (2016). Microfluidic Based Hydrate Permeability System: Design and Construction, West Virginia University.

Tohidi, B., R. Anderson, M. B. Clennell, R. W. Burgass and A. B. Biderkab (2001). 'Visual observation of gas-hydrate formation and dissociation in synthetic porous media by means of glass micromodels.' Geology 29(9): 867-870.

Wang, S., Z. Cheng, Q. Liu, P. Lv, J. Lv, L. Jiang and Y. Song (2021). 'Microscope insights into gas hydrate formation and dissociation in sediments by using microfluidics.' Chemical Engineering Journal 425: 130633.

Xu, R., X. Kou, T.-W. Wu, X.-S. Li and Y. Wang (2023). 'Pore-scale experimental investigation of the fluid flow effects on methane hydrate formation.' Energy: 126967.

Zhang, J., N. Zhang, X. Sun, J. Zhong, Z. Wang, L. Hou, S. Li and B. Sun (2023). 'Pore-scale investigation on methane hydrate formation and plugging under gas–water flow conditions in a micromodel.' Fuel 333: 126312.